Metabolic Engineering 78 (2023) 61–71

Contents lists available at ScienceDirect

Metabolic Engineering

journal homepage: www.elsevier.com/locate/meteng

"*In vivo* biosynthesis of *N,N*-dimethyltryptamine, 5-MeO-*N,N*-dimethyltryptamine, and bufotenine in *E. coli*"

Lucas M. Friedberg [a,1], Abhishek K. Sen [a], Quynh Nguyen [a], Gabriel P. Tonucci [b], Elle B. Hellwarth [a], William J. Gibbons Jr. [a], J. Andrew Jones [a,*]

[a] *Miami University, Department of Chemical, Paper, and Biomedical Engineering, Oxford, OH, 45056, USA*
[b] *Miami University, Department of Microbiology, Oxford, OH, 45056, USA*

ARTICLE INFO

Keywords:
DMT
Psychedelic
5-MeO-DMT
Bufotenine
Colorado river toad
Indolethylamine-*N*-Methyltransferase

ABSTRACT

N,N-dimethyltryptamine (DMT), 5-methoxy-*N,N*-dimethyltryptamine (5-MeO-DMT) and 5-hydroxy-*N,N*-dimethyltryptamine (bufotenine) are psychedelic tryptamines found naturally in both plants and animals and have shown clinical potential to help treat mental disorders, such as anxiety and depression. Advances in both metabolic and genetic engineering make it possible to engineer microbes as cell factories to produce DMT and its aforementioned derivatives to meet demand for ongoing clinical study. Here, we present the development of a biosynthetic production pathway for DMT, 5-MeO-DMT, and bufotenine in the model microbe *Escherichia coli*. Through the application of genetic optimization techniques and process optimization in benchtop fermenters, the *in vivo* production of DMT in *E. coli* was observed. DMT production with tryptophan supplementation reached maximum titers of 74.7 ± 10.5 mg/L under fed batch conditions in a 2-L bioreactor. Additionally, we show the first reported case of *de novo* production of DMT (from glucose) in *E. coli* at a maximum titer of 14.0 mg/L and report the first example of microbial 5-MeO-DMT and bufotenine production *in vivo*. This work provides a starting point for further genetic and fermentation optimization studies with the goal to increase methylated tryptamine production metrics to industrially competitive levels.

1. Background and Introduction

N,N-dimethyltryptamine (DMT) is a tryptophan-derived alkaloid that is naturally present in many plants and animals. As a structural analog of serotonin, DMT acts as an agonist to 5-HT_{2A} serotonin receptors in the brain, inducing acute, hallucinogenic, mind-altering changes. DMT has a thousand-year history of being consumed by several indigenous groups from the Northwestern Amazon for therapeutic purposes (Miller et al., 2019; Schultes et al., 2001). Indigenous groups orally ingested a DMT-containing mixture called ayahuasca, which is made from the leaves of the shrub *Psychotria viridis,* the source of DMT, and the vine *Banisteriopsis caapi*, the source of monoamine oxidase inhibitors (MAOIs) required for DMT to be orally active (Schultes et al., 2001). The pioneering work of Richard Manske, Oswaldo Gonclaves de Lima, and Stephen Szara resulted in the development of a chemical synthesis route (Manske, 1931), linked DMT to its natural occurrence in plants (de Lima, 1946), and connected DMT with its hallucinogenic properties (Szára, 1956), respectively. The discoveries made by the aforementioned scientists led to a link between modern science and the historical use of DMT in religious and spiritual practices rooted in the mind-altering effects of the chemical.

Similarly, DMT derivatives, 5-methoxy-*N,N*-dimethyltryptamine (5-MeO-DMT), and its active metabolite 5-hydroxy-*N,N*-dimethyltryptamine (5-HO-DMT, or bufotenine) exhibit hallucinogenic properties upon parenteral administration. These compounds have been traced back thousands of years for their use in ceremonies in Central and South America in the form of crushed seeds known as 'Yopo' and through the parotoid gland secretions of the Colorado River Toad, *Incilius alvarius* (Carod-Artal and Vázquez Cabrera, 2007; Shen et al., 2010).

Clinical depression is a highly prevalent and debilitating disorder estimated to affect 4.4% of the global population (World Health Organization, 2017). Recently, psychoactives, such as DMT, 5-MeO-DMT, MDMA, ketamine, and psilocybin, have gained interest as potential alternatives to traditional Selective Serotonin Reuptake Inhibitor

* Corresponding author. Miami University, 64P Engineering Building, 650 E. High St. Oxford, OH, 45056, USA.
E-mail addresses: lucasfriedberg@gmail.com (L.M. Friedberg), sena2@miamioh.edu (A.K. Sen), nguyenq3@miamioh.edu (Q. Nguyen), tonuccgp@miamioh.edu (G.P. Tonucci), hellwae@miamioh.edu (E.B. Hellwarth), gibbonwj@miamioh.edu (W.J. Gibbons), jonesj28@miamioh.edu (J.A. Jones).
[1] Current address: National Renewable Energy Laboratory, Golden, CO 80401.

https://doi.org/10.1016/j.ymben.2023.05.006
Received 11 February 2023; Received in revised form 15 May 2023; Accepted 22 May 2023
Available online 23 May 2023

(SSRI)-based antidepressants such as fluoxetine (Prozac®). In an open-label clinical trial held at Universidade de Sao Paulo, Ribeirao Preto, Brazil, 6 patients were administered ayahuasca and showed significant reductions in their depressive scores of up to 82% based on the Hamilton Rating Scale for Depression (HAM-D) and the Montgomery-Asberg Depression Rating Scale (MADRS)(de Osório et al., 2015). A recent study has surveyed over 10,000 global ayahuasca users on the negative side-effects of use, with up to 70% of users reporting minor adverse effects (e.g., vomiting) while under the influence (Bouso et al., 2022). These adverse effects were generally not significant enough to halt future use, indicating that the users felt the benefits of use outweighed any potential harm (Bouso et al., 2022). It is important to note that these studies were performed with ayahuasca, not pharmaceutical-grade drug product, but the frequency of adverse effects is sufficient to warrant further study to explore the safety and efficacy of this powerful class of drug candidates. With growing evidence to support DMT's use as an effective, long-term anti-depressant, there is a growing need to develop sustainable, reproducible, and scalable synthesis methods to provide a safe source for pharmaceutical-grade product.

In 1961, the discovery of methylated tryptamines produced by a cytosolic S-adenosyl-L-methionine (SAM)-dependent methyltransferase was described in the rabbit lung (Axelrod, 1961). Further studies observed the production of *N*-methyltryptamine (NMT) and DMT in human and rat brain incubated with tryptamine, revealing the presence of indolethylamine-*N*-methyltransferase (INMT) activity (Mandell and Morgan, 1971; Saavedra et al., 1973). In 1999, human INMT (hINMT) was successfully cloned, further elucidating the broad presence of methylated tryptamines in human physiology and metabolism (Thompson et al., 1999).

Recently, phenylalkylamine *N*-methyltransferase (PaNMT) from *Ephedra sinica* has demonstrated a broad range of substrate promiscuity *in vitro* ranging from its native substrate, norephedrine, to indoleamines (Morris et al., 2018). Fig. 1 displays the core tryptamine structure common to the neurotransmitter serotonin and to some psychedelics such as DMT and psilocybin.

Here we demonstrate *in vivo* activity of *Homo sapiens* INMT and *Ephedra sinica* PaNMT in an *E. coli* host, resulting in the production of NMT, DMT, and *N,N,N*-trimethyltryptamine (TMT) from tryptamine. We also demonstrate the incorporation of these enzymes into functional metabolic pathways to realize methylated tryptamine biosynthesis from a variety of substrates, including tryptophan and indole derivatives. Fig. 2 illustrates the novel pathway for methylated tryptamine biosynthesis through the simultaneous enzymatic expression of both the tryptophan decarboxylase from *Psilocybe cubensis*, PsiD (Fricke et al., 2017), and INMT or PaNMT coupled with the native *E. coli* metabolism.

Combinatorial metabolic engineering is a proven technique to quickly sample the transcriptional design space for a pathway and find optimal expression levels (Naseri and Koffas, 2020; Young et al., 2021). Several DNA assembly methods and modular parts have been reported including Golden Gate (Engler et al., 2008), BioBricks (Knight, 2003), Gibson Assembly (Gibson et al., 2009), and CRISPR-mediated (Shola et al., 2020) approaches, yet we chose ePathOptimize (J Andrew Jones et al., 2015), because it allows for the randomization of parts in various genetic architectures and is compatible with existing pathway modules developed in our lab (Adams et al., 2019, 2022).

Libraries of transcriptionally varied genetic mutants of both PsiD and INMT were constructed using the ePathOptimize approach and screened using a medium throughput, pH-controlled, well plate platform coupled with HPLC-MS analysis (Adams et al., 2019; J Andrew Jones et al., 2015). Further analysis of fermentation conditions identified pH and temperature as key process parameters, which was consistent with previous results reported in the literature for *in vitro* approaches (Morris

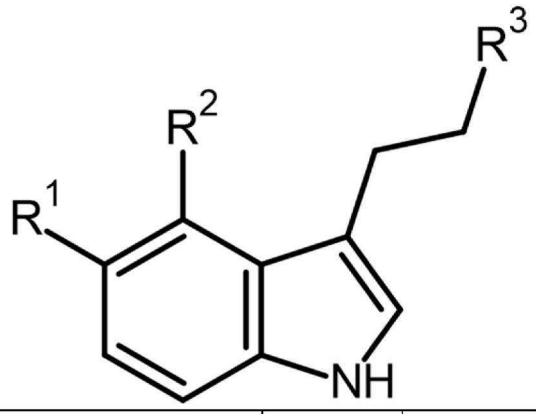

Name	R^1	R^2	R^3
Tryptamine	-H	-H	$-NH_2$
N-methyltryptamine (NMT)	-H	-H	$-NH(CH_3)$
N,N-dimethyltryptamine (DMT)	-H	-H	$-N(CH_3)_2$
N,N,N-trimethyltryptamine (TMT)	-H	-H	$-N(CH_3)_3^+$
5-methoxy-DMT (5-MeO-DMT)	$-O(CH_3)$	-H	$-N(CH_3)_2$
Bufotenine (5-HO-DMT)	-OH	-H	$-N(CH_3)_2$
Psilocin	-H	-OH	$-N(CH_3)_2$
Psilocybin	-H	$-OPO_3H^-$	$-NH(CH_3)_2^+$
Serotonin (5-HO-tryptamine)	-OH	-H	$-NH_2$

Fig. 1. Chemical structures and names of common, bioactive tryptamines.

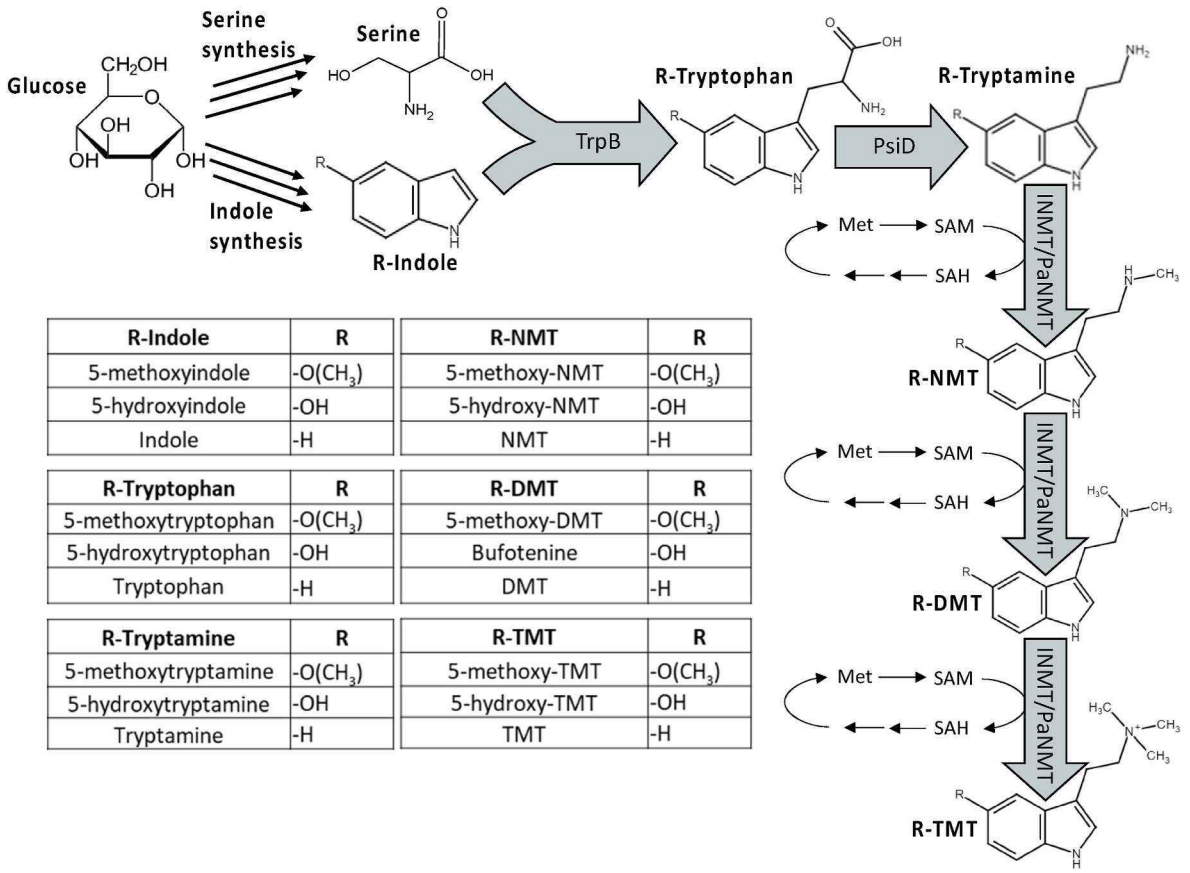

R-Indole	R	R-NMT	R
5-methoxyindole	-O(CH_3)	5-methoxy-NMT	-O(CH_3)
5-hydroxyindole	-OH	5-hydroxy-NMT	-OH
Indole	-H	NMT	-H

R-Tryptophan	R	R-DMT	R
5-methoxytryptophan	-O(CH_3)	5-methoxy-DMT	-O(CH_3)
5-hydroxytryptophan	-OH	Bufotenine	-OH
Tryptophan	-H	DMT	-H

R-Tryptamine	R	R-TMT	R
5-methoxytryptamine	-O(CH_3)	5-methoxy-TMT	-O(CH_3)
5-hydroxytryptamine	-OH	5-hydroxy-TMT	-OH
Tryptamine	-H	TMT	-H

Fig. 2. Metabolic pathway for the production of *N*-methylated tryptamines from various starting substrates. TrpB = tryptophan synthase, β-subunit; PsiD = tryptophan decarboxylase; INMT = indolethylamine-*N*-methyltransferase; PaNMT = phenylalkylamine-*N*-methyltransferase; SAM = S-Adenosyl methionine (cosubstrate); SAH = S-Adenosyl homocysteine; Met = methionine; NMT = *N*-methyltryptamine; DMT = *N,N*-dimethyltryptamine; TMT = *N,N,N*-trimethyltryptamine.

et al., 2018).

Using the novel pathway outlined in Fig. 2, indole derivatives such as 5-methoxyindole and 5-hydroxyindole are converted to psychoactive derivatives of DMT, specifically 5-MeO-DMT and bufotenine, respectively, through leveraging INMT and PsiD substrate promiscuity. Furthermore, we have shown that genetic and fermentation optimization led to a substantial increase in DMT titers from initial proof of concept experiments, leading to the first example of *de novo* production of DMT in *E. coli*.

2. Results

2.1. Temperature and pH dependent production of DMT

Both methyltransferases investigated in this study, INMT and PaNMT, were expressed in *E. coli* using the strong consensus T7-*lac* promoter system. The production of NMT and DMT by these recombinant *E. coli* hosts were monitored as a function of both temperature and pH. The pathway intermediate, tryptamine, was provided in the culture media to allow for the direct assessment of effective methyltransferase activity. Induction with IPTG led to the biosynthesis of NMT and DMT in INMT expressing cultures, and only NMT in PaNMT expressing cultures under standard screening conditions. DMT was never observed in the absence of NMT. Supplementary Fig. 1a provides a qualitative visual for the time variant pH levels throughout this assay. The highest titers observed for both NMT and DMT in initial 48-well plate experiments (7.6 ± 0.5 mg/L and 0.2 ± 0.01 mg/L, respectively) were observed in INMT expressing *E. coli* at 42 °C with an initial media pH of 8.0 (Fig. 3bc). NMT and DMT concentrations were significantly higher in cultures incubated with a starting pH of 8 compared to other pHs tested ($p < 0.05$) (Fig. 3). In PaNMT expressing *E. coli*, NMT titer reached a high of 1.2 ± 0.003 mg/L when grown at 30 °C and having the media pH initially adjusted to 8 (Fig. 3a). DMT production was not observed in PaNMT expressing *E. coli* under these conditions. The 150 mg/L tryptamine supplementation was not exhausted during these studies. NMT and DMT titers from the expression of INMT were highest at temperatures of 42 °C, whereas PaNMT expression had its highest NMT titers at 30 °C.

2.2. Promoter library screening under monitored pH helps identify most suitable promoter

Following the trends observed from the temperature and pH-dependent production of NMT and DMT, we screened a panel of transcriptionally varied mutants to select genetically superior strains for methylation of tryptamine. A promoter library was screened for both INMT and PaNMT expressing plasmids. IPTG inducible promoters from the weakest to strongest (G6, H9, H10, C4, and T7) and constitutive promoters (XylA and GAP) were all independently tested (J Andrew Jones et al., 2015; Jones et al., 2017; Xu et al., 2014). Methylated tryptamine production was tested by culturing cells in a media at pH 7.5 and 42 °C with 150 mg/L supplementary tryptamine. In order to compensate for the decrease in pH over time (Supplementary Fig. 1a), we readjusted the pH to 7.5 every 2 h over the course of 10 h following the pH-controlled methods as represented in Supplementary Fig. 1b. Despite large variability in production across the tested strains, the original consensus T7-based construct resulted in the highest concentrations of both NMT and DMT. NMT and DMT production from INMT under the control of the T7 consensus promoter reached titers of 3.6 ± 0.1 mg/L and 2.5 ± 0.1 mg/L, respectively (Supplementary Fig. 2a).

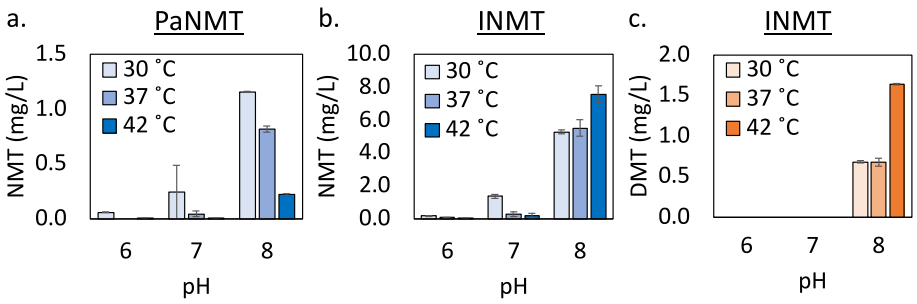

Fig. 3. NMT and DMT concentrations from BL21 Star™ (DE3) expressing INMT or PaNMT in 48-well plates after 24 h under standard screening conditions. a) NMT produced by PaNMT expressing strain as a function of temperature and pH. b) NMT produced by INMT expressing strain as a function of temperature and pH. c) DMT produced by PaNMT expressing strain as a function of temperature and pH. Under each condition, 150 mg/L of tryptamine was initially supplemented in the fermentation media. No DMT observed in PaNMT screening. Error bars represent ± one standard deviation from the mean of duplicate samples.

PaNMT production of NMT was also highest under T7 consensus-facilitated expression with titers reaching 0.3 ± 0.03 mg/L (Supplementary Fig. 2b). These results led to the use of the T7 promoter for all further experimentation with INMT and PaNMT, single-gene constructs.

2.3. Strict pH monitoring and control increases NMT and DMT production

With the results from the temperature, pH, and genetic optimization assays for methylated tryptamine production completed, we next scaled up production through the use of a bioreactor, which allowed us to maintain a constant pH throughout the fermentation (Supplementary Fig. 1c). We used BL21 Star™ (DE3) containing pETM6-SDM2x-INMT (T7 promoter) as our model bioreactor strain due to its consistently higher concentrations of both NMT and DMT as compared to PaNMT in previous well plate studies. Production of NMT, DMT, and TMT was measured, at pH 6.5, 7.0, 7.5, and 8.0 (Fig. 4). For all three methylated tryptamine compounds of interest (NMT, DMT, and TMT), fermentations conducted under pH-stat conditions of pH = 7.5 yielded the highest titers. NMT titers from pH 7.5 fermentations reached 11.4 ± 2.0 mg/L, a 1.5-fold increase over highest NMT titers observed from the previous 48-well plate assays. DMT titers from pH 7.5 fermentations reached 12.7 ± 3.3 mg/L, which represents a 7.8-fold increase compared to DMT produced from the top performing 48-well plate assays. TMT titers were also observed in the largest quantities from the pH 7.5 fermentations at a value of 6.8 ± 2.5 mg/L, representing the first TMT production observed from a bacterial culture.

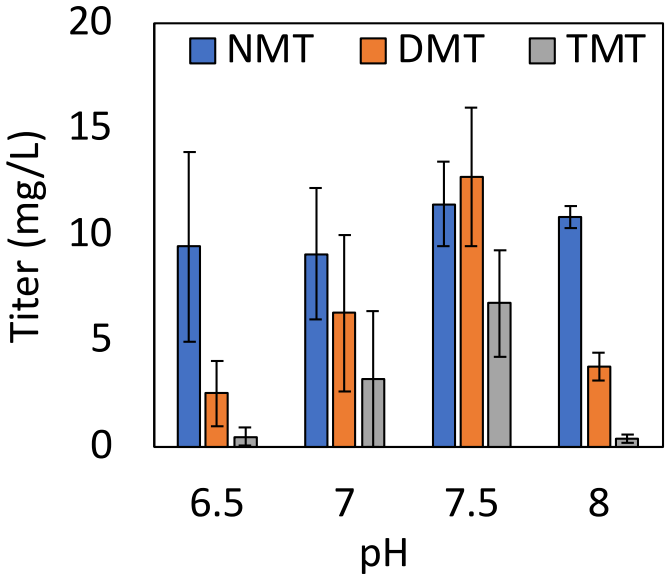

Fig. 4. NMT, DMT, and TMT production from 150 mg/L of tryptamine under pH stat bioreactor conditions using the BL21 Star™ (DE3) strain containing pETM6-SDM2x-INMT. Highest concentrations of NMT, DMT, and TMT were achieved at pH = 7.5. Error bars represent ± one standard deviation from the mean of two or more samples.

2.4. Extended metabolic pathways and further promoter library screening lead to de novo production of methylated tryptamine

We further explored the synthesis of DMT from tryptophan by extending our metabolic pathway to include PsiD, a tryptophan decarboxylase native to the psilocybin biosynthesis pathway of *Psilocybe cubensis*. This extended pathway enables a theoretical *de novo* pathway to methylated tryptamines from glucose in *E. coli* (Fig. 2).

Initial studies, including promoter library optimization, were conducted in tryptophan-supplemented media to reduce metabolic burden and show proof of concept of the newly constructed metabolic pathway. All promoter library screens were performed using the pH-controlled, medium-throughput, screening assay (Supplementary Fig. 1b). Lead strains from the promoter library screens were selected for their ability to produce the highest titers of DMT from tryptophan. The selected strains were then used to test the viability of *de novo* DMT biosynthesis. Fig. 5 illustrates the outcome of the promoter library screening, resulting in a pathway construct capable of producing more DMT from tryptophan as compared to the T7-INMT-PsiD expressing strain. The T7-INMT-PsiD strain was created as an initial proof of concept for *de novo* production of DMT and has been labeled to easily compare its performance within the promoter library screening results. All two-gene, transcriptional library constructs are expressed from a single plasmid. Fig. 5a shows the combined results of two separate promoter library screens with varied operon gene orientation, specifically, xx5-PsiD-INMT and xx5-INMT-PsiD. A total of 96 random mutants were selected with 48 strains selected per operon gene orientation. The 'xx5' notation indicates the pseudorandom incorporation of 5 mutant T7 promoters of varied strength. Given the large number of strains that need to be screened for promoter library representation, strains were tested in singlicate (n = 1), and lead mutants were later isolated and rescreened in replicate. Fig. 5b represents the monocistronic library screen of 144 strains for the gene orientation INMT-PsiD (xx5-INMT-xx5-PsiD). Within the operon, monocistronic, and pseudooperon (xx5-psiD-xx5-INMT) promoter libraries, the best performing strains resulted in just under 25 mg/L DMT and NMT (Fig. 5a–c). The highest TMT titer was observed just under 12 mg/L within the monocistronic promoter library (Fig. 5b). The pseudooperon library screening results represented in Fig. 5d (144 strains screened) reveal that the INMT-PsiD gene expression order was less successful compared to the pseudooperon library screening counterpart, PsiD-INMT, as seen in Fig. 5c (144 strains screened). The INMT-PsiD gene expression order was the least successful overall in providing high DMT-producing strains compared to the other configurations.

Fig. 6a shows the comparison in DMT production between top-to middle-performing strains selected from each promoter library screening in Fig. 5. Strains represented in Fig. 6 were labeled and identified according to the promoter library they were selected from, and the number that was assigned during initial screening: M =

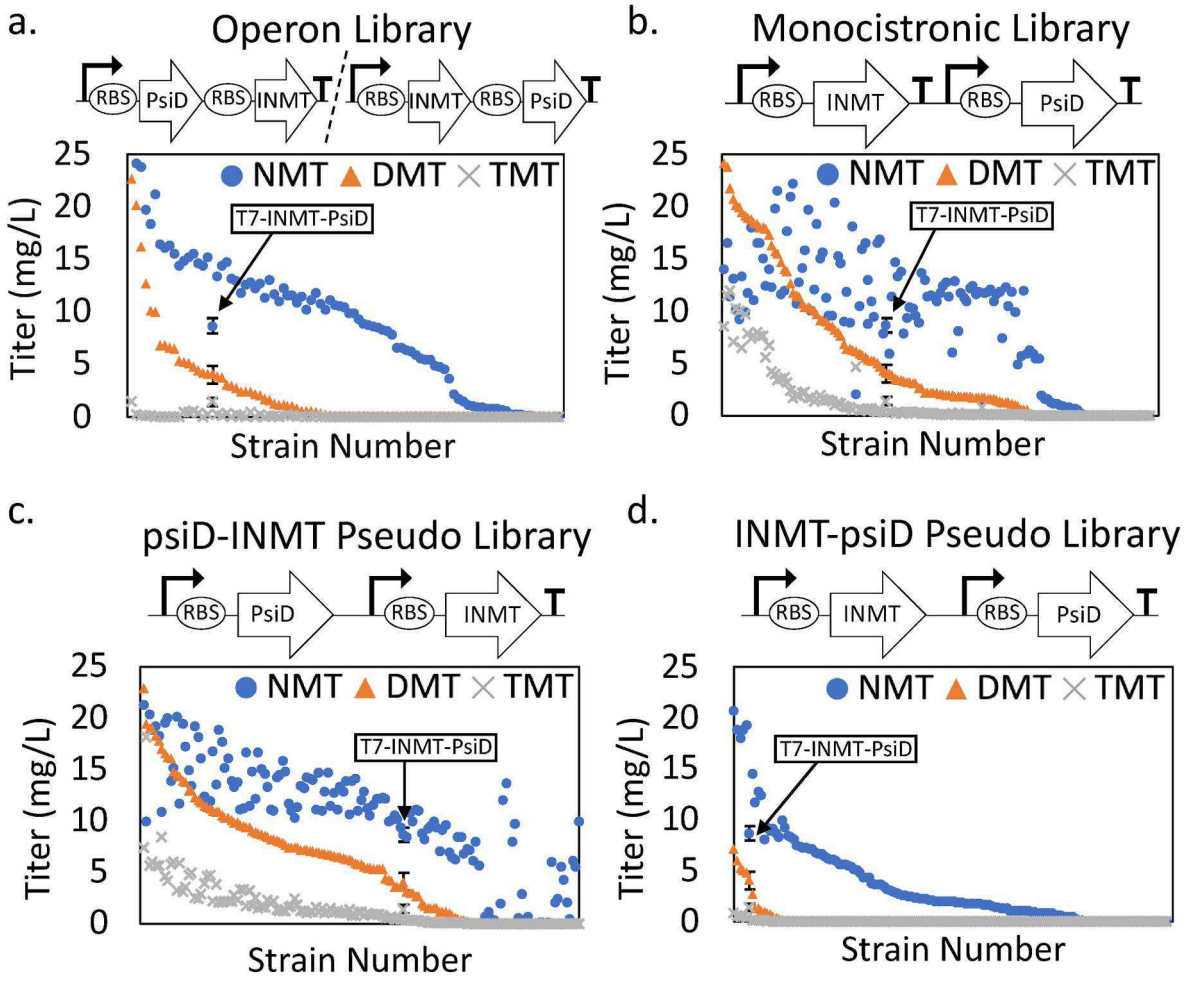

Fig. 5. NMT, DMT, and TMT concentrations for promoter engineered constructs containing INMT and PsiD, arranged in order of decreasing DMT concentrations. a) Operon configuration: xx5-INMT-PsiD and xx5-PsiD-INMT, b) Monocistronic configuration: xx5-INMT-xx5-PsiD, c) Pseudooperon configuration: xx5-PsiD-xx5-INMT, d) Pseudooperon configuration: xx5-INMT-xx5-PsiD.

monocistronic, P = pseudooperon, O = operon. T7-INMT-PsiD (T7-I-D) was again used as a baseline comparison for the success of the promoter library in increasing DMT titers. All strains, with the exception of M29, O20, and M132 produced significantly more DMT than T7-INMT-PsiD ($p < 0.05$). Strains M111, M21, P117, P29, and O1 were selected for all future methylation screenings to represent a range of top performers from basic operon, pseudooperon, and monocistronic pathway configurations. All lead strains were sent for sequencing to determine the promoter identities controlling the expression of psiD and INMT. These results revealed a broad range of promoter strengths with the top strains generally containing weakened T7 mutant promoters (G6, H9, and H10), with a few exceptions. Additionally, 4 populations of replicate strains were identified, as noted in Fig. 6a, with genetically identical strains performing similarly in all cases.

These top strains were also tested for their ability to catalyze *de novo* biosynthesis (Fig. 6b). Screening conditions were conserved from previous studies; however, tryptophan was not supplemented into the media, such that glucose represents the sole carbon source for growth and product formation. All selected promoter library strains produced significantly more DMT ($p < 0.05$) than the T7-INMT-PsiD strain, with the M111 strain producing 14.0 ± 0.4 mg/L DMT and 31.3 ± 0.8 mg/L of total methylated tryptamines (Fig. 6b).

2.5. Bioreactor fermentation with glucose feed increases DMT titers

Benchtop bioreactor fermentation was carried out similarly to previously described bioreactor methods but with the addition of a glucose feed and DO cascade, which previously went unused as initial studies used a pH-controlled batch operation paradigm. With the addition of a glucose-fed batch strategy, we revisited the viability of DMT production scale-up; as a result, we chose our T7-INMT strain with tryptamine supplementation at both 37 °C and 42 °C to compare directly to previous bioreactor data (Supplementary Fig. 3). Additionally, we compared the DMT production outputs of the T7-INMT strain with tryptamine supplementation to genetically optimized strains that contained both INMT and PsiD with tryptophan supplementation, strains M111 and P117. Supplementary Fig. 3 shows the end point NMT, DMT, and TMT titers observed under a glucose-fed batch condition. Strains M111 and P117 were grown in Andrew's Magic Media (AMM) supplemented with 1 g/L of tryptophan. Strain T7-INMT was grown in AMM supplemented with 150 mg/L tryptamine. T7-INMT produced more DMT when the fermentation was run at 42 °C compared to 37 °C, although this difference was not significant ($p > 0.05$). The addition of the glucose feed made a significant difference in DMT production from tryptamine (Fig. 4 vs. Supplementary Fig. 3), showing a 3-fold increase in DMT production ($p < 0.01$). Furthermore, both M111 and P117 were able to produce more methylated tryptamines from tryptophan than the T7-INMT strain from tryptamine under fed batch conditions, suggesting the methyltransferase step to be rate limiting. M111 produced 74.7 ± 10.5 mg/L of DMT and 192.0 ± 17.0 mg/L total methylated tryptamines, representing the highest DMT titers reported to date for a recombinant organism. A representative profile of methylated tryptamine

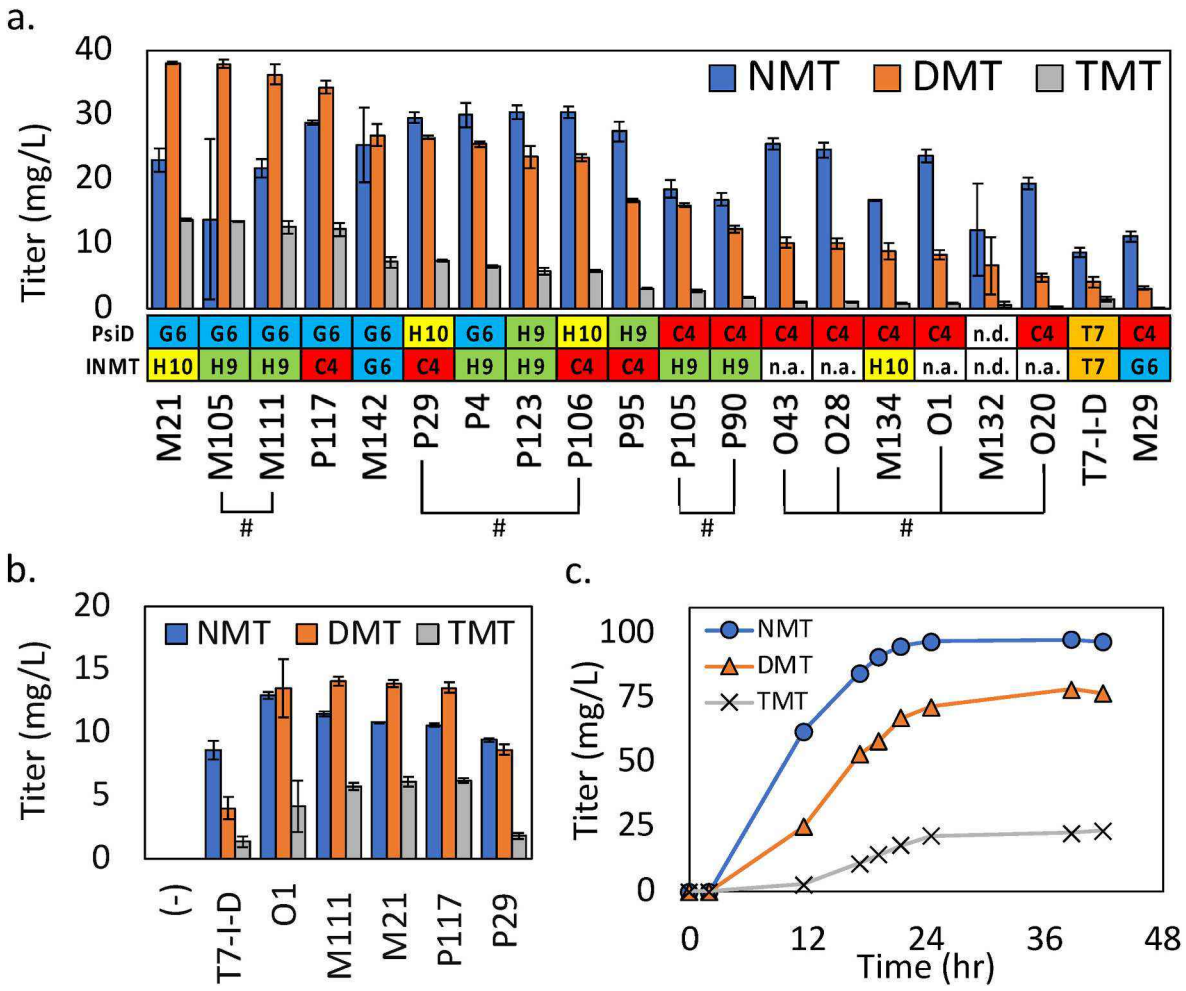

Fig. 6. Rescreening of transcriptionally optimized strains. a) NMT and DMT production of selected strains from each distinct library construct. Strain: M = monocistronic, P = pseudooperon, O = operon. Promoter identity is shown below the horizontal axis. Strains with identical promoter identities signified by a pound sign (#). n.a., not applicable (operon strains only contain a single promoter); n.d., not determined (this strain was not able to be revived from permanent storage). Promoter strengths have been previously reported from low to high: G6 (blue), H9 (green), H10 (yellow), T7 (orange), C4 (red). b) *De novo* production (from glucose) of NMT, DMT, and TMT by select lead strains. c) Representative 2-liter bioreactor production profile for optimized strain M111 supplemented with 1 g/L tryptophan. (−) symbolizes the negative control empty vector. T7-I-D = T7-INMT-PsiD. Error bars represent ± one standard deviation from the mean of (a) triplicate (b) duplicate samples.

production by strain M111 under glucose-fed batch conditions is presented in Fig. 6c.

2.6. Production of 5-MeO-DMT and bufotenine

By leveraging the substrate promiscuity of both PsiD and INMT in tandem with *E. coli*'s native tryptophan synthase β-subunit, TrpB, we

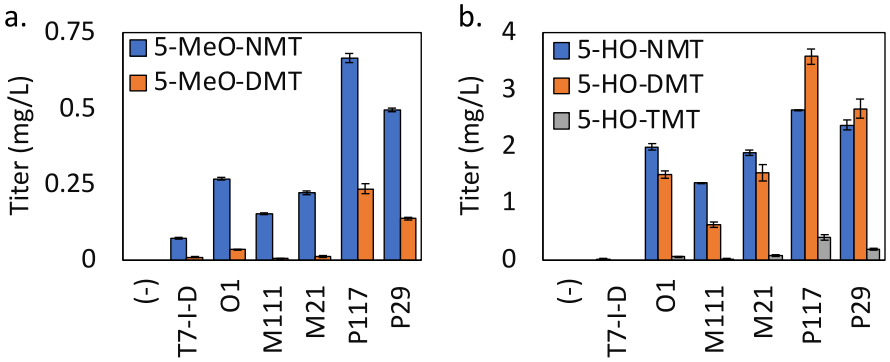

Fig. 7. Production of 5-methoxy- and 5-hydroxy-DMT derivatives. a) 5-MeO-NMT and 5-MeO-DMT production by select strains. No 5-MeO-TMT was observed. b) 5-HO-NMT, 5-HO-DMT, and 5-HO-TMT production. (−) symbolizes the negative control empty vector. T7-I-D = T7-INMT-PsiD. Error bars represent ± one standard deviation from the mean of duplicate samples.

demonstrated that our production platform could process indole derivatives 5-methoxyindole (5-MeO-indole) and 5-hydroxyindole (5-HO-indole) into DMT derivatives 5-MeO-DMT and bufotenine, respectively. Native TrpB expression and substrate flexibility was sufficient to process the externally supplemented indole derivatives into tryptophan derivative intermediate products, these were then acted on by the previously described DMT pathway enzymes. Strains selected for this screening were the same as used for the *de novo* production of DMT. The pH-controlled, medium-throughput, screening method was used to realize the production of both of these DMT derivatives. Fig. 7a shows the production of 5-MeO-NMT and 5-MeO-DMT by select strains with strain P117 producing the maximum observed titers of 0.7 ± 0.02 mg/L and 0.2 ± 0.02 mg/L, respectively. Fig. 7b shows the production of 5-hydroxy-methylatedtryptamines by strain P117 with maximum observed titers of 2.6 ± 0.003 mg/L, 3.5 ± 0.02 mg/L, and 0.4 ± 0.05 mg/L of 5-HO-NMT, bufotenine, and 5-HO-TMT, respectively.

2.7. Evaluation of in situ product removal to enhance DMT production

Through the studies outlined above, we have shown that DMT and DMT derivatives can be synthesized *in vivo*; however, the bioreactor fermentation studies indicate that limitations in this biosynthetic production platform of DMT exist. The presence of unmethylated tryptamine in the LCMS analysis corroborates the idea that INMT methylation of tryptamine is the rate limiting step for the *in vivo* biosynthesis of DMT and DMT derivatives described in this work. Chu et al. (2014), suggest that the activity of INMT is attenuated by both noncompetitive and competitive inhibition of DMT on the methyltransferase (Chu et al., 2014). *In situ* removal of DMT could alleviate this potential inhibition of INMT (Freeman et al., 1993). To test this hypothesis, we screened two potential hydrophobic overlays (dodecane and diisononyl phthalate) as a potential sink for DMT during fermentation. Unfortunately, we observed minimal partition of methylated tryptamines into either hydrophobic overlay, limiting our ability to reduce any INMT inhibition that may be present. More thorough study using a more diverse range of hydrophobic overlays may provide valuable insight into an appropriate path towards enhanced fermentation-based production of methylated tryptamines.

3. Discussion

This study shows the first reported case of *in vivo* NMT, DMT, and TMT production, as well as their 5-methoxy and 5-hydroxy derivatives, using a prokaryotic host. Human INMT was selected for this study based on literature reports of activity on tryptamine substrates dating back over 60 years (Axelrod, 1961), with more recent studies demonstrating active recombinant production in eukaryotic hosts (Thompson et al., 1999). PaNMT was selected based on one previous report (Morris et al., 2018) which demonstrated low-level promiscuous activity towards tryptamines. With no known homologs being previously studied, we elected to use the PaNMT sequence which was previously reported to have low activity. Additionally, this study demonstrates the effectiveness of optimizing genetic and fermentation conditions for the purpose of enhancing desired product titers; however, the fermentation-based process still requires further improvements before an industrially competitive bioprocess will become a reality.

It was possible to identify key parameters for successful methylated tryptamine biosynthesis through the use of 48-well plate assays. HPLC-MS analysis enabled the identification of desired products within the culture media, confirming the presence of NMT, DMT, and TMT. This validated the hypothesis that INMT and PaNMT could be used to enable *in vivo* methylation of tryptamine in *E. coli*.

Identifying the optimal pH and temperature for INMT and PaNMT methylation activity led to a large increase in product titers over traditional *E. coli* batch fermentation conditions of 37 °C at a neutral initial pH that is not strictly controlled. By employing stricter limits on pH fluctuation over time, final titers of NMT and DMT were increased compared to cultures without pH control (Figs. 4 and 3bc). We observed consistent trends in INMT methylation activity with respect to temperature and pH; however, PaNMT activity remained unpredictable due to low yields, with NMT and DMT concentrations frequently near the limit of quantification (Fig. 3a). The PaNMT-containing *E. coli* strain was less successful in producing both NMT and DMT compared to the strain containing INMT, under their respective optimal conditions. Furthermore, our *in vivo* results show PaNMT activity decreasing at elevated fermentation temperature (Fig. 3a), which was not expected as PaNMT activity was previously reported to increase with temperature in an *in vitro* system up to approximately 52 °C (Morris et al., 2018). The reasoning behind the discrepancy between *in vitro* and *in vivo* temperature optimums is currently unknown, but it is important to note that the previous report measured the temperature optimum on the less bulky phenylalkylamine substrate, norephedrine, which may account for the discrepancy between studies.

Genetic optimization through the testing of a wide range of different strength promoters, including both inducible and constitutive expression, demonstrated the efficacy of the strongly inducible T7 promoter in the production of NMT, DMT, and TMT from tryptamine (Supplementary Fig. 2). It is important to note that although the initial screening demonstrated a clear preference for the T7 promoter, it will be imperative that extended pathways be rescreened via the pH-controlled medium-throughput, well plate assay described above. As the biosynthesis pathway is extended, the metabolic burden and associated co-factor and precursor needs from the native *E. coli* metabolism will change, directly affecting the interplay between expression level for the exogenous pathway and resource availability for endogenous metabolism (Wu et al., 2016).

Scaled-up production to benchtop fermenters proved successful as INMT methylation of tryptamine was seen to increase as observed through enhanced titers of NMT, DMT, and the first observation of TMT biosynthesis (Fig. 4). It is important to note that the only variables monitored and controlled through the initial use of benchtop fermenters were the pH, maintained at 7.5, and the temperature, controlled at 42 °C. Dissolved oxygen (DO), an integral parameter for maximizing cell growth and maintaining ideal fermentation conditions, was not monitored or controlled, leaving room for future bioreactor-based optimization studies. It should also be addressed that the TMT identified in the bioreactor studies presented above has not been well described in terms of its potential psychoactive effects and to our knowledge has only previously been described twice in the peer-reviewed literature (Servillo et al., 2012). Due to the structural similarity to the natural product, aeruginascin, it is expected that TMT may have bioactivity motivating further study to enhance its production and exploration of its pharmacological potential in animal studies. Furthermore, the biosynthesis of NMT, DMT, and most notably, TMT, was observed to be catalyzed by the human INMT, indicating that these mono- and tri-methylated derivatives may play a currently unstudied role in human health. The development of an *E. coli*-based process to facilitate the efficient biosynthesis of these compounds can lead to more focused studies to determine the roles and mechanism of actions for tryptamines in human neurobiology.

A total of six lead plasmid constructs were selected from an iterative screening process of each transcriptionally varied library to be further tested for their ability to produce DMT from either tryptophan or glucose (Fig. 5). The *de novo* biosynthesis of DMT was attempted in this study to eliminate the need for relatively more expensive substrates such as tryptophan, tryptamine, serine, or indole, compared with D-glucose. Through the expression of transcriptionally varied genetic mutants of PsiD and INMT onto a single plasmid construct using the ePathOptimize transcriptional optimization approach (J Andrew Jones et al., 2015), we were able to achieve *de novo* production of NMT and DMT *in vivo* (Fig. 6b). Final data analysis led to the identification of the top *de novo* performing strain M111, which contains a monocistronic gene construct

with the low strength T7 mutant promoters H9 and G6 controlling the expression of INMT and PsiD, respectively (H9-INMT-G6-PsiD). Through screening of genetically varied libraries, we were able to demonstrate the first example of a microbe capable of *de novo* (from glucose) synthesis of NMT, DMT, and TMT in a bacterial host platform. Out of the five lead variants selected after screening of the ePathOptimize libraries, we found a range of promoters present, ranging from our weakest (G6) to our strongest (C4) promoter (Supplementary Table 1, Plasmids #13–17). This observation combined with the promoter sensitivity observed within each library (Fig. 5), suggests that different pathway architectures resulted in the selection of different 'best' promoter strengths. Future studies focused on understanding the global context of pathway optimization are necessary to fully explain this observation (J. A. Jones et al., 2015; Wu et al., 2016).

Native *E. coli* TrpB, and heterologous PsiD and INMT were shown to exhibit substrate promiscuity through the production of 5-MeO-DMT and bufotenine via the metabolic pathway described in Fig. 2. 5-MeO-DMT and bufotenine are both psychoactive DMT derivatives that reside in some species of plants and the Colorado River Toad, native to the Sonoran Desert. These compounds have recently seen increased use recreationally and spiritually and have anecdotally been known to help treat mental health conditions (Davis et al., 2019). The same elite performing strains isolated for the *de novo* production of DMT were used for this screening process. Results led to the identification of strain P117, which contains a pseudooperon gene construct with the weak G6 promoter controlling the expression of PsiD and the strong C4 promoter controlling INMT expression (G6-PsiD-C4-INMT), as the most effective strain in producing both 5-MeO-DMT and bufotenine from their respective indole precursors (Fig. 7). After producing DMT derivatives we believed that we could further use the observed substrate promiscuity in attempt to produce psilocin (4-HO-DMT), the active form of the native mushroom psychedelic, psilocybin, by feeding the substrate 4-hydroxyindole using the same pathway previously described. Unfortunately, we were unable to detect any presence of psilocin in our fermentation media (data not shown). The substrate promiscuity demonstrated by the production of these DMT analogs suggests that additional DMT derivatives, both existing and novel, could be produced through this metabolic pathway. The limited evidence presented here suggests there will likely be some chemical position sensitivity; however, screening of different promoter variants and/or enzyme homologs from varied species may be able to overcome this limitation.

In conclusion, the biosynthesis of DMT through application of metabolic and pathway engineering principles in *E. coli* presented in this work is the first instance of *in vivo* and *de novo* DMT synthesis in a prokaryotic host. The highest titer of DMT achieved in this study is reported as 74.7 ± 10.5 mg/L, which was synthesized by a recombinant *E. coli* strain co-expressing the human INMT and *Psilocybe cubensis* PsiD from tryptophan-supplemented media. The reported maximum molar yield on supplemented tryptophan was 0.081 mol/mol for DMT and 0.215 mol/mol for total methylated tryptamines. Further genetic optimization efforts to enhance the *de novo* DMT synthesis pathway, and to tailor the fermentation process to enhance DMT production, could lead to an alternative production method competitive with the chemical synthesis of DMT (Cozzi and Daley, 2020; Speeter and Anthony, 1954). As regulations around the studies of DMT and its derivatives for medical use continue to relax, it is important that avenues for the controlled supply and discovery of these medicinal compounds are continuously explored (Gibbons et al., 2021).

4. Materials and methods

4.1. Bacterial strains, vectors and media

E. coli DH5α was used to propagate all plasmids, while BL21 Star™ (DE3) was used as the host for all chemical production experiments. Plasmid transformations were completed using standard chemical competency protocols. Unless otherwise noted, Andrew's Magic Media (AMM) (He et al., 2015) (without MOPS and tricine), was supplemented with 1.0 g/L methionine and 150 mg/L of tryptamine or 1 g/L tryptophan and 100 mg/L of alternative precursor molecules such as 5-hydroxyindole, or 5-methoxyindole depending on the desired end product (Fig. 2). Tryptophan (1 g/L) was provided in a greater excess than tryptamine (150 mg/L) or alternative indole precursors (100 mg/L) because the *E. coli* host is expected to utilize tryptophan for protein synthesis as well as target product synthesis, while tryptamine and the indole derivatives have no metabolic uses in *E. coli* outside of target product synthesis. The supplement concentrations were chosen to provide sufficient substrate across the range of scales (2-mL well plate to 2-L bioreactor) studied in this work. Nonsupplemented AMM was used for preculture growth while supplemented AMM was used for production media (He et al., 2015). Luria Broth (LB) was used for plasmid propagation during cloning. The antibiotic ampicillin (80 μg/mL) was added to the culture media when appropriate for plasmid selection. The exogenous pathway gene encoding PsiD was taken from a plasmid construct reported by the Jones Lab for psilocybin biosynthesis (Adams et al., 2019).

4.2. Plasmid construction

Human INMT and PaNMT gene sequences were ordered as linear, double-stranded DNA fragments from Genewiz Inc. (now Azenta). INMT and PaNMT were codon optimized for expression in *E. coli*, PCR-amplified with primers containing restriction sites *Nde*I and *Xho*I, and ligated into a modified ePathBrick expression vector also digested with *NdeI* and *XhoI* (Adams et al., 2019). The resulting plasmids containing the genes responsible for INMT and PaNMT expression, #4 and #5 respectively, were sequence-verified and used to create all pathway variants and transcriptionally varied libraries described below. All multigene expression plasmids were constructed using the previously published ePathBrick methods as described above, while all transcriptional libraries were constructed using standard ePathOptimize methods and mutant T7 promoters G6, H9, H10, and C4 to create operon and pseudooperon configurations for plasmids #6 and #7 and a monocistronic configuration for plasmid #5 (J Andrew Jones et al., 2015; Xu et al., 2012). Additional information on plasmids constructed for this study can be found in Supplementary Table 1.

4.3. Standard screening conditions

Standard screening was performed in 2 mL working volume cultures in 48-well plates at either 30, 37, or 42 °C, depending on gene construct. Nonsupplemented AMM was used for overnight cultures, and AMM supplemented with the relevant precursor molecules was used for production cultures. Overnight cultures were grown either from agar plates or glycerol freezer stocks in AMM (pH = 7.0) with appropriate antibiotics for 12–16 h in a shaking (250 rpm) incubator at 30, 37, or 42 °C. Production cultures were inoculated at 2% of working volume (40 μL into 2 mL) with the overnight cultures grown under similar process conditions. Cultures were grown with a minimum number of replicates of N = 2, unless otherwise noted. Induction with 1 mM isopropyl β-D-1-thiogalactopyranoside (IPTG) occurred 4h after inoculation unless otherwise noted. Cultures were then sampled for HPLC and LCMS analysis 24 h post inoculation.

4.4. Initial pH screening method

The standard screening method outlined above was used with the addition of varying the initial pH condition. The overnight cultures were grown using the conditions outlined above to result in a standardized inoculum. Before inoculation, the AMM supplemented with 150 mg/L tryptamine, 1.0 g/L methionine, and ampicillin was pH-adjusted to either 7.0, 7.5, or 8.0 using 1 M KOH, or to 6.0 or 6.5 using 1 M HCl.

Fermentation pH was not monitored throughout the fermentation, and conditions correspond to those outlined in the standard screening method above.

4.5. pH-controlled, medium-throughput, screening method

Using the standard screening conditions described above, we developed a modified protocol to test chemical production under pH-controlled conditions in a medium-throughput, well plate screening approach. Replicate 48-well plates were set up in a way to allow for many replicate cultures, which could be sacrificed for pH monitoring and empirical pH adjustment purposes. Beginning at time of induction (4 h post inoculation), 4 mL (2 mL from 2 sacrificial wells) of the pH control plate were transferred into a 15 mL conical tube, and the pH was measured using a Fisher Scientific Accumet™ AE150 pH benchtop meter. pH of the sacrificial culture was then adjusted by the addition of 10 M KOH in 2 μL increments until the desired setpoint was achieved. pH at the time of sampling averaged about 6.7 and required, on average, 15 μL of 10 M KOH. The total volume of 10 M KOH required was recorded and used to inform the adjustment of the pH, using a 2.5 M KOH solution, for the remaining sacrificial controls and experimental cultures in the 48-well plate format. The pH measuring and adjustment procedure described above was performed every 2 h over the course of 8 h beginning at induction unless otherwise noted.

4.6. Promoter library validation

Upon constructing and testing promoter library strains, freezer stock cultures were made by combining cultures grown overnight with 30% sterile glycerol to produce a final 15% glycerol stock in sterile 96-well plates. Once promoter library constructs were screened using the previously mentioned screening methods, a few top-performing strains, based on DMT titer, from each library were selected for further screening. Selected strains were streaked from previously described freezer stock plates onto an agar plate containing ampicillin. The following day, streaked plates were used to inoculate a 48-well plate for screening. Immediately following inoculation, an agar plate containing ampicillin was patched to preserve mutants for future study and permanent storage. Once strain performance was validated in replicate, select mutants from the agar plate were grown overnight in AMM. Plasmid DNA of overnight cultures was isolated and purified using Omega Bio-tek E.Z.N.A.® Plasmid DNA Mini Kit, followed by digestion and gel electrophoresis to confirm expected plasmid construct. Purified plasmid DNA was then transformed into *E. coli* DH5α and plated on agar plates containing ampicillin. Colonies of transformants were used to grow overnight cultures in LB. DH5α overnight cultures were subjected to plasmid DNA purification, followed by sequence verification using restriction enzyme digestion and Sanger sequencing. Verified plasmid DNA was transformed back into BL21 Star™ (DE3). Transformants were grown overnight in AMM. Overnight cultures were used to create permanent freezer stocks, which served as the final production strain moving forward with additional screening.

4.7. pH stat bioreactor screening

Once optimal conditions were determined using our standard and pH-controlled screening conditions at both 37 °C and 42 °C, we selected the Eppendorf BioFlo120 bioreactor with a 1.5 L working volume to scale up DMT production. The cylindrical vessel was mixed by a direct drive shaft containing two Rushton-type impellers. The overnight culture of BL21 Star™ (DE3) containing pETM6-SDM2x-INMT was grown for 12 h at 37 °C in 50 mL of AMM supplemented with methionine (1 g/L), tryptamine (150 mg/L), and ampicillin (80 μg/mL) in a 250 mL nonbaffled Erlenmeyer flask. The bioreactor contained the same media composition that was used for the overnight culture and was inoculated at a 2% v/v (30 mL into 1.5 L). Temperature was held at a constant 42 °C with a heat jacket and recirculating cooling water; pH was automatically and continuously controlled at 6.5, 7.0, 7.5, or 8.0, with the addition of 10 M KOH. Agitation and air flow rate were maintained at 500 rpm and 2 v/v (3 SLPM) for the entirety of the 24-h fermentation. Samples were collected periodically for measurement of OD_{600} and metabolite analysis. The fermentation cultures were induced 4 h post-inoculation with 1.0 mM IPTG using an IPS series laboratory syringe pump (Inovenso, IPS-14RS). Apart from periodic sample collection, the reactor screening process required minimal observation with integrated control systems sensing and maintaining process parameters as described above. The concentration of DMT and all metabolic intermediates and side products were analyzed via HPLC and LCMS.

Final bioreactor fermentations reported in Fig. 6c and Supplementary Fig. 3 were carried out with the addition of a 50% w/v glucose feed and DO cascade control (30% of saturation) to agitation (300–1000 rpm). Glucose analysis was performed using an Aminex HPX-87H column maintained at 30 °C followed by a refractive index detector (RID) held at 35 °C. The mobile phase was 5 mM H_2SO_4 in water at a flow rate of 0.6 mL/min. Glucose was quantified using a standard curve with a retention time of 8.8 min (Adams et al., 2019).

4.8. Analytical methods

Samples were prepared for HPLC and LCMS analysis by centrifugation at 21,000 rcf for 5 min; 2 μL of the resulting supernatant was then injected for analysis. Analysis was performed on a Thermo Scientific Ultimate 3000 High-Performance Liquid Chromatography (HPLC) system equipped with Diode Array Detector (DAD) and Thermo Scientific ISQ™ EC single quadrupole mass spectrometer (MS).

Mass spectroscopy extracted ion channels (EIC) were used in tandem with UV absorbance at 280 nm to quantify the aromatic compounds of interest in this study. Metabolite separation was performed using an Agilent Zorbax Eclipse XDB-C18 analytical column (3.0 mm × 250 mm, 5 μm) with mobile phases of water (A) and acetonitrile (B) both containing 0.1% formic acid at a rate of 1 mL/min: 0 min, 5% B; 0.43 min, 5% B; 5.15 min, 19% B; 6.44 min, 100% B; 7.73 min, 100% B; 7.73 min, 5% B; 9.87 min, 5% B (Adams et al., 2022). The ISQ™ EC mass spectrometer, equipped with a heated electrospray ionization (HESI) source, was operated in positive mode. The mass spectrometer was supplied ≥99% purity nitrogen using a Peak Scientific Genius XE 35 laboratory nitrogen generator. The source and detector conditions were as follows: sheath gas pressure of 80.0 psig, auxiliary gas pressure of 9.7 psig, sweep gas pressure of 0.5 psig, foreline vacuum pump pressure of 1.55 Torr, vaporizer temperature of 500 °C, ion transfer tube temperature of 300 °C, source voltage of 3049 V, source current of 15.90 μA.

LCMS data was collected, where the full MS scan was used to provide an EIC of our compounds of interest for the DMT production platform (M+1): tryptamine (m/z 161), NMT (m/z 175), DMT (m/z 189), and TMT (m/z 203). This method resulted in the following observed retention times as verified by analytical standards (when commercially available): tryptamine (5.63 min), NMT (5.79 min), DMT (6.01 min) and TMT (6.05 min).

EICs for compounds of interest for the 5-MeO-DMT production platform (M+1): 5-MeO-tryptamine (m/z 191), 5-MeO-NMT (m/z 205), 5-MeO-DMT (m/z 219). This method resulted in the following observed retention times as verified by analytical standards (when commercially available): 5-MeO-tryptamine (5.98 min), 5-MeO-NMT (6.34 min) and 5-MeO-DMT (6.59 min). 5-MeO-TMT was not observed.

EICs for compounds of interest for the bufotenine production platform (M+1): 5-HO-tryptamine (m/z 177), 5-HO-NMT (m/z 191), bufotenine (m/z 205), 5-HO-TMT (m/z 219). This method resulted in the following observed retention times as verified by analytical standards (when commercially available): 5-HO-tryptamine (2.87 min), 5-HO-NMT (3.27 min), bufotenine (3.53 min), and 5-HO-TMT (3.49 min).

All data was managed and processed using Thermo Scientific Chromeleon 7.3 Chromatography Data System.

4.9. Analytical method validation for DMT, 5-MeO-DMT, and bufotenine

Quantification using absorbance in the ultraviolet region could not be solely used in this study due to difficulty achieving separation of *N,N*-dimethyl and *N,N,N*-trimethyl metabolites by liquid chromatography. Supplementary Figs. 4 and 5 provide a visual representation of NMT, DMT, and TMT retention as compared with a DMT standard. This complication led to the use of absorbance at 280 nm for the quantification of NMT titer and the sum of DMT/TMT titer, while the ratio of the peak areas from mass spectroscopy EICs for DMT and TMT were used to partition the DMT/TMT peak area.

DMT analytical standard was purchased from Cerilliant Corporation. The authentic standard was used to create a series of standard curves through serial dilution in spent and filtered cell broth, and these samples were analyzed to validate the methods described above. Several DMT standard curves were run to validate quantification by tandem A280-LCMS using EICs: (1) A bioreactor broth sample containing NMT, DMT, and TMT was serially diluted in a broth that was free of DMT. Each diluted sample was spiked with an additional 40 mg/L of pure DMT to ensure that saturation of DMT would not affect the quantification of TMT in the diluted samples (Supplementary Fig. 6a), and (2) A bioreactor broth sample containing NMT, DMT, and TMT was serially diluted in a negative control cell broth to confirm that the ratio of DMT:TMT remained consistent over a wide range of analyte concentrations (Supplementary Fig. 6b). Each validation test provided good alignment with expected results and the presence of saturating amounts of DMT did not affect NMT or TMT quantification. We used the ratio of DMT:TMT EIC peak areas and area from the A280 chromatogram to quantify NMT, DMT, and TMT products on a DMT molar basis due to the absence of commercially available standards for NMT and TMT.

5-MeO-DMT and bufotenine standard curves were created via serial dilutions of 1.0 mg/mL pure reagent stock solutions purchased from Cerilliant and Lipomed respectively. The quantification of respective products was performed as described above for NMT, DMT, and TMT.

5. Statistical methods

Two-tailed, unpaired t-tests with 95% confidence intervals were performed for all claims of significance throughout the manuscript. All experimental results were performed in duplicate, unless otherwise noted.

Author contributions

JAJ and LMF designed the study. All authors performed experiments. JAJ secured the funding for the project. LMF, EBH, and JAJ analyzed data. LMF and JAJ wrote the manuscript. All authors edited and reviewed the manuscript prior to submission.

Declaration of competing interest

JAJ is the chairman of the scientific advisory board and a significant stakeholder at PsyBio Therapeutics. PsyBio Therapeutics has licensed tryptamine biosynthesis-related technology from Miami University. JAJ, WJGJ, and LMF are co-inventors on several related patent applications. All other authors declare no conflicts of interest.

Data availability

Data will be made available on request.

Acknowledgments

This work was supported by a sponsored research grant from PsyBio Therapeutics (JAJ). Requests for strains and plasmids capable of producing controlled substances (e.g., DMT, bufotenin, and 5-MeO-DMT) will require proof of appropriate approvals and licenses from all necessary state and federal agencies prior to completion of a materials transfer agreement. The authors would also like to thank Alexandra M. Adams for assistance with initial molecular cloning of INMT and PaNMT, and David K. Tiller for helpful comments and discussions on the final draft.

Appendix A. Supplementary data

Supplementary data to this article can be found online at https://doi.org/10.1016/j.ymben.2023.05.006.

References

Adams, A.M., Anas, N.A., Sen, A.K., Hinegardner-Hendricks, J.D., O'Dell, P.J., Gibbons, W.J., Flower, J.E., McMurray, M.S., Jones, J.A., 2022. Development of an E. coli-based norbaeocystin production platform and evaluation of behavioral effects in rats. Metab. Eng. Commun. 14 https://doi.org/10.1016/j.mec.2022.e00196.

Adams, A.M., Kaplan, N.A., Wei, Z., Brinton, J.D., Monnier, C.S., Enacopol, A.L., Ramelot, T.A., Jones, J.A., 2019. In vivo production of psilocybin in E. coli. Metab. Eng. 56, 111–119. https://doi.org/10.1016/J.YMBEN.2019.09.009.

Axelrod, J., 1961. Enzymatic Formation of psychotomimetic metabolites from normally occurring compounds. Science. https://doi.org/10.1126/science.134.3475.343, 1979) 134, 343–343.

Bouso, J.C., Andión, Ó., Sarris, J.J., Scheidegger, M., Tófoli, L.F., Opaleye, E.S., Schubert, V., Perkins, D., 2022. Adverse effects of ayahuasca: results from the global ayahuasca survey. PLOS Glob. Pub. Health 2, e0000438. https://doi.org/10.1371/journal.pgph.0000438.

Carod-Artal, F.J., Vázquez Cabrera, C.B., 2007. Ritual use of Anadenanthera seeds among South America natives. Neurologia 22, 410–415.

Chu, U.B., Vorperian, S.K., Satyshur, K., Eickstaedt, K., Cozzi, N.v., Mavlyutov, T., Hajipour, A.R., Ruoho, A.E., 2014. Noncompetitive inhibition of indolethylamine-N-methyltransferase by N, N-dimethyltryptamine and N, N-dimethylaminopropyltryptamine. Biochemistry 53, 2956–2965. https://doi.org/10.1021/bi500175p.

Cozzi, N.v., Daley, P.F., 2020. Synthesis and characterization of high-purity N,N-dimethyltryptamine hemifumarate for human clinical trials. Drug Test. Anal. 12, 1483–1493. https://doi.org/10.1002/dta.2889.

Davis, A.K., So, S., Lancelotta, R., Barsuglia, J.P., Griffiths, R.R., 2019. 5-methoxy-N,N-dimethyltryptamine (5-MeO-DMT) used in a naturalistic group setting is associated with unintended improvements in depression and anxiety. Am. J. Drug Alcohol Abuse 45, 161–169. https://doi.org/10.1080/00952990.2018.1545024.

de Lima, O.G., 1946. Observações sobre o "vinho da Jurema" utilizado pelos índios Pancarú de Tacaratú (Pernambuco). Separata dos Arquivos Do I. P. A. 4, 45–80.

de Osório, F.L., Sanches, R.F., Macedo, L.R., dos Santos, R.G., Maia-De-Oliveira, J.P., Wichert-Ana, L., de Araujo, D.B., Riba, J., Crippa, J.A., Hallak, J.E., 2015. Antidepressant effects of a single dose of ayahuasca in patients with recurrent depression: a preliminary report. Rev. Bras. Psiquiatr. 37, 13–20. https://doi.org/10.1590/1516-4446-2014-1496.

Engler, C., Kandzia, R., Marillonnet, S., 2008. A one pot, one step, precision cloning method with high throughput capability. PLoS One 3, e3647. https://doi.org/10.1371/JOURNAL.PONE.0003647.

Freeman, A., Woodley, J.M., Lilly, M.D., 1993. In situ product removal as a tool for bioprocessing. Nat. Biotechnol. 11, 1007–1012.

Fricke, J., Blei, F., Hoffmeister, D., 2017. Enzymatic synthesis of psilocybin. Angew. Chem. Int. Ed. 56, 12352–12355. https://doi.org/10.1002/anie.201705489.

Gibbons, W.J., McKinney, M.G., O'Dell, P.J., Bollinger, B.A., Jones, J.A., 2021. Homebrewed psilocybin: can new routes for pharmaceutical psilocybin production enable recreational use? Bioengineered 12, 8863–8871. https://doi.org/10.1080/21655979.2021.1987090.

Gibson, D.G., Young, L., Chuang, R.-Y., Venter, J.C., Hutchison, C.A., Smith, H.O., 2009. Enzymatic assembly of DNA molecules up to several hundred kilobases. Nat. Methods 6, 343–345. https://doi.org/10.1038/nmeth.1318.

He, W., Fu, L., Li, G., Andrew Jones, J., Linhardt, R.J., Koffas, M., 2015. Production of chondroitin in metabolically engineered E. coli. Metab. Eng. 27 https://doi.org/10.1016/j.ymben.2014.11.003.

Jones, J.A., Toparlak, T.D., Koffas, M.A.G., 2015. Metabolic pathway balancing and its role in the production of biofuels and chemicals. Curr. Opin. Biotechnol. 33, 52–59. https://doi.org/10.1016/j.copbio.2014.11.013.

Jones, J.A., Vernacchio, V.R., Collins, S.M., Shirke, A.N., Xiu, Y., Englaender, J.A., Cress, B.F., McCutcheon, C.C., Linhardt, R.J., Gross, R.A., Koffas, M.A.G., 2017. Complete biosynthesis of anthocyanins using E. coli polycultures. mBio 8, e00621. https://doi.org/10.1128/mBio.00621-17, 17.

Jones, J Andrew, Vernacchio, V.R., Lachance, D.M., Lebovich, M., Fu, L., Shirke, A.N., Schultz, V.L., Cress, B., Linhardt, R.J., Koffas, M.A.G., 2015. ePathOptimize: a combinatorial approach for transcriptional balancing of metabolic pathways. Sci. Rep. 5, 11301 https://doi.org/10.1038/srep11301.

Knight, T., 2003. Idempotent Vector Design for Standard Assembly of Biobricks.

Mandell, A.J., Morgan, M., 1971. Indole(ethyl)amine N-methyltransferase in human brain. Nat. New Biol. 230, 85–87.

Manske, R.H.F., 1931. A synthesis of the methyltryptamines and some derivatives. Can. J. Res. 5, 592–600. https://doi.org/10.1139/cjr31-097.

Miller, M.J., Albarracin-Jordan, J., Moore, C., Capriles, J.M., 2019. Chemical evidence for the use of multiple psychotropic plants in a 1,000-year-old ritual bundle from South America. Proc. Natl. Acad. Sci. U. S. A. 166, 11207–11212. https://doi.org/10.1073/pnas.1902174116.

Morris, J.S., Groves, R.A., Hagel, J.M., Facchini, P.J., 2018. An n-methyltransferase from ephedra sinica catalyzing the formation of ephedrine and pseudoephedrine enables microbial phenylalkylamine production. J. Biol. Chem. 293, 13364–13376. https://doi.org/10.1074/jbc.RA118.004067.

Naseri, G., Koffas, M.A.G., 2020. Application of combinatorial optimization strategies in synthetic biology. Nat. Commun. https://doi.org/10.1038/s41467-020-16175-y.

Saavedra, J.M., Coyle, J.T., Axelrod, J., 1973. The distribution and properties of the nonspecific N-methyltransferase in brain. J. Neurochem. 20, 743–752. https://doi.org/10.1111/J.1471-4159.1973.TB00035.X.

Schultes, R.E., Hofmann, A., Rätsch, C., 2001. Plants of the Gods: Their Sacred, Healing, and Hallucinogenic Powers, second ed. Healing Arts Press, Rochester, VT. 10.3/JQUERY-UI.JS.

Servillo, L., Giovane, A., Balestrieri, M.L., Cautela, D., Castaldo, D., 2012. N-methylated tryptamine derivatives in citrus genus plants: identification of N, N, N -trimethyltryptamine in bergamot. J. Agric. Food Chem. 60, 9512–9518. https://doi.org/10.1021/jf302767e.

Shen, H.-W., Jiang, X.-L., Winter, C.J., Yu, A.-M., 2010. Psychedelic 5-methoxy-N,N-dimethyltryptamine: metabolism, pharmacokinetics, drug interactions, and pharmacological actions. Curr. Drug Metabol. 11, 659–666.

Shola, D.T.N., Yang, C., Kewaldar, V.S., Kar, P., Bustos, V., 2020. New additions to the CRISPR toolbox: CRISPR-CLONInG and CRISPR-CLIP for donor construction in genome editing. CRISPR J. 3, 109–122. https://doi.org/10.1089/CRISPR.2019.0062/ASSET/IMAGES/LARGE/CRISPR.2019.0062_FIGURE6.JPEG.

Speeter, M.E., Anthony, W.C., 1954. The action of oxalyl chloride on indoles: a new approach to tryptamines. J. Am. Chem. Soc. 76, 6208–6210.

Szára, S., 1956. Dimethyltryptamin: its metabolism in man; the relation of its psychotic effect to the serotonin metabolism. Experientia 12, 441–442. https://doi.org/10.1007/BF02157378.

Thompson, M.A., Moon, E., Kim, U.-J., Xu, J., Siciliano, M.J., Weinshilboum, R.M., 1999. Human indolethylamine N-methyltransferase: cDNA cloning and expression, gene cloning, and chromosomal localization. Genomics 61, 285–297.

World Health Organization, 2017. Depression and Other Common Mental Disorders Global Health Estimates.

Wu, G., Yan, Q., Jones, J.A., Tang, Y.J., Fong, S.S., Koffas, M.A.G., 2016. Metabolic burden: cornerstones in synthetic biology and metabolic engineering applications. Trends Biotechnol. https://doi.org/10.1016/j.tibtech.2016.02.010.

Xu, P., Li, L., Zhang, F., Stephanopoulos, G., Koffas, M., 2014. Improving fatty acids production by engineering dynamic pathway regulation and metabolic control. Proc. Natl. Acad. Sci. U. S. A. 111, 11299–11304. https://doi.org/10.1073/pnas.1406401111.

Xu, P., Vansiri, A., Bhan, N., Koffas, M.A.G., 2012. ePathBrick: a synthetic biology platform for engineering metabolic pathways in E. coli. ACS Synth. Biol. 1, 256–266. https://doi.org/10.1021/sb300016b.

Young, R., Haines, M., Storch, M., Freemont, P.S., 2021. Combinatorial metabolic pathway assembly approaches and toolkits for modular assembly. Metab. Eng. https://doi.org/10.1016/j.ymben.2020.12.001.